Phase Composition-Microstructure-Thermal Conductivity Relationships in MgO-$Nd_2Zr_2O_7$ Composite Inert Matrix Materials

LA-UR 09-06689

Approximately 2000 metric tons of plutonium from spent nuclear fuel and dismantled nuclear weapons exists in stockpiles worldwide. Furthermore, 70 to 80 metric tons of plutonium and other minor actinides (neptunium, americium and curium) are added each year. These stockpiles can be reduced through actinide transmutation and Pu burning in nuclear reactors. This process currently incorporates fissile materials into a MOX fuel which is then burned in a light water reactor (LWR). Unfortunately, MOX fuels hold fissile materials in a U-238 matrix in order to dilute them to the volumetric concentrations required by reactor control considerations. During reactor operation, neutron capture by this matrix produces plutonium as a waste product.

Currently, a neutron-transport inert matrix (IM) material is being developed as a replacement for the MOX fuel matrix. In order to be approved for use in LWRs by regulatory commissions, the IM material must meet five criteria:

- High thermal conductivity
- High radiation resistance
- Compatibility with reactor materials
- Favorable neutronics
- Suitability for either direct disposal or reprocessing

This research focuses on thermal conductivity quantification of various phase compositions of an MgO-$Nd_2Zr_2O_7$ composite IM material. By relating the phase composition of the IM to its microstructural and thermal properties, we hope to collect data which will, along with that gathered on its performance with respect to the other criteria, allow us to determine the optimal composition of this material.

When the IM is combined with a fissile phase, an inert matrix fuel (IMF) is obtained. The non-fertile IM does not cause plutonium breeding through neutron capture. With a simulated net reduction in plutonium of 80-90% by volume during standard LWR operation, IMFs have the potential to greatly increase the efficiency of nuclear material disposal.
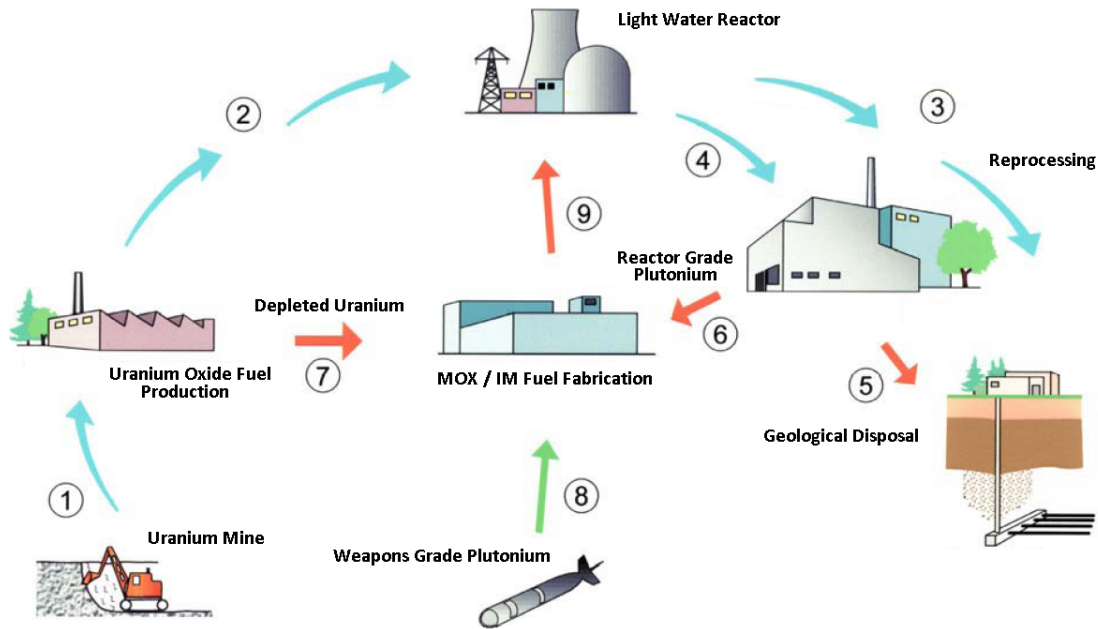
**Fig. 1**: The fuel cycle used in the recycling, burning, and transmutation of actinides.

**Materials Selection**

Two oxides, $ZrO_2$ and MgO, have been widely studied as possible IM materials. Similar materials such as Zircaloy and Magnox have been successfully used in LWRs, however, both fail to meet at all the criteria necessary for regulatory approval. Zirconia has low thermal conductivity, which has resulted in the creation of a large temperature gradient within fuel pellets during testing. This can result in a pellet centerline temperature close to the liquidus temperature of the IMF. Magnesia has high thermal conductivity, but is incompatible with the coolant used in LWRs. In normal reactor, the IMF would not contact the coolant due to the use of cladding. However, in the event of a cladding failure, the hydration and subsequent corrosion of the magnesia phase would compromise the integrity of the fuel pellet.
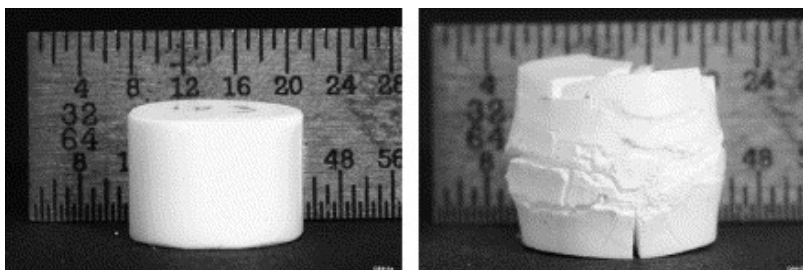


**Fig. 2**: A magnesia pellet before and after immersion in boiling water for 3 hours.

A composite approach using an Mgo- $ZrO_2$ material has been shown to exhibit both high thermal conductivity and suitable hot water corrosion resistance. The thermally conductive MgO phase, as long

as it possesses suitable contiguity, serves as a heat flow path. The zirconia phase significantly slows the corrosion of the magnesia phase through the following mechanism.

Hydration of MgO begins at its grain boundaries. The reaction between water and magnesia, forming $Mg(OH)_2$, is accompanied by a volume increase of 117%. This increase in volume at the grain boundaries exerts stress on neighboring grains. In pure magnesia, this would create cracks at which further hydration and volume increase occurs. The addition of a $ZrO_2$ phase reduces the area of MgO exposed to hydration attack at the grain boundaries, while also reducing the stress placed on MgO grains. As a result, cracking of the MgO phase does not occur. Without the production of new hydration-vulnerable cracks, the hydration process is dramatically slowed.



**Fig. 3**: The hydration attack and corrosion process of an MgO-$ZrO_2$ composite. (a) the hydration attack begins at MgO grain boundaries. The red arrows denote stress placed on grains due to the volume increase which accompanied the production of magnesium hydroxide. (b) Without cracking in the MgO grains, the corrosion process occurs as a slow, uniform removal of material. (c) This corrosion continues until a layer of MgO grains has been removed. (d) As the MgO grains are removed, $ZrO_2$ grains are as well.
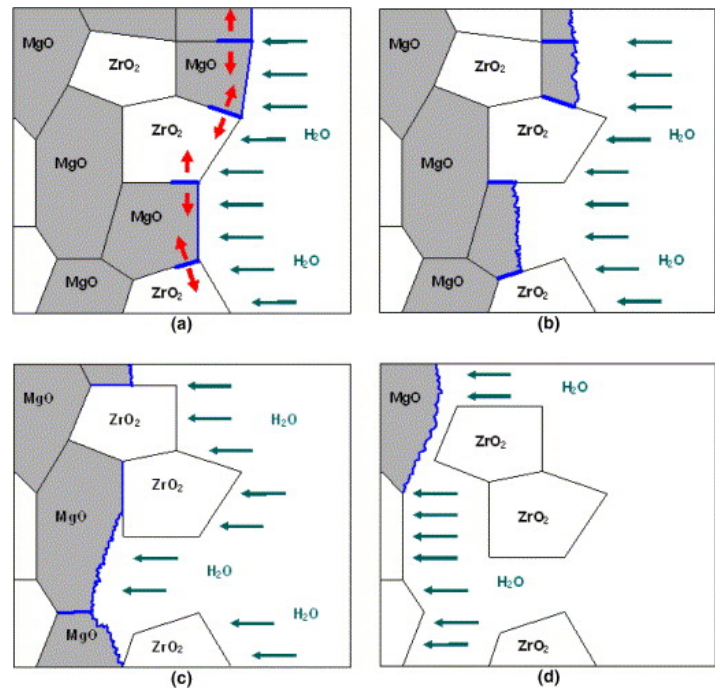
It has been found that an MgO-$Nd_2Zr_2O_7$ composite performs similarly to this material in terms of hot water corrosivity, while offering slightly higher thermal conductivity. Other pyrochlores tested as zirconia substitutes include $La_2Zr_2O_7$ and $Pr_2Zr_2O_7$, but both of these materials decayed to the fluorite crystal lattice structure during irradiation.

**Objectives**

In previous work, various processing methods for a 70 vol% MgO / 30 vol% $Nd_2Zr_2O_7$ composite were tested in order to determine the relationships between processing, microstructure, and thermal conductivity. The 70/30 composition was chosen because Monteburns simulations showed that a 50/50 composition had a lower than ideal neutron multiplication factor while a 90/10 concentration would

require the use of a neutron poison. The processing methods tested include: mortar and pestle grinding, magnetic bar stirring, spex blending,and ball milling.

It was concluded that Ball milling produced the most consistency with respect to microstructural and thermal properties. In this work, we are testing MgO-Nd$_2$Zr$_2$O$_7$ composites of various compositions to determine the relationship between phase composition, microstructure, and thermal conductivity.  We are using the processing methods previously developed. The compositions being tested are: 70/30, 60/40, 50/50, and 40/60.
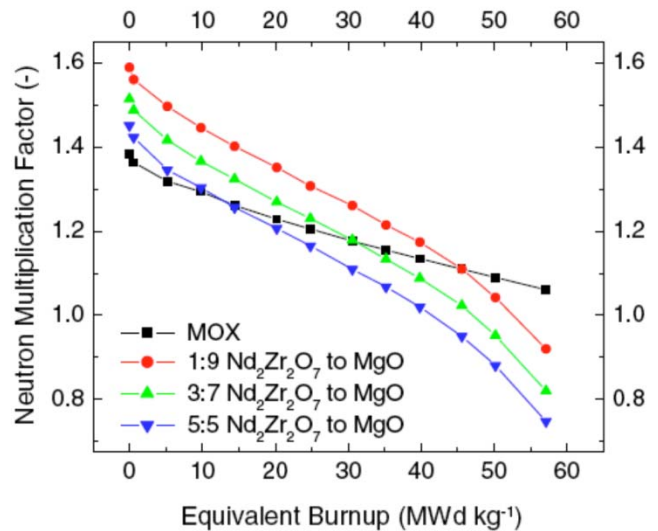


**Fig. 4**: The relationships between phase composition, neutron multiplication factor, and equivalent burnup in the MgO-Nd2Zr2O7 composite as determined by Monteburns simulations.

**Processing**

The following methods are being used to synthesize the MgO and Nd$_2$Zr$_2$O$_7$ powders used in this work and to fabricate the composite pellets.

Commercially received MgO (Cerac 99.95%):

- Calcined in air for 2 hours at 1000°C.

Stoichiometric ratios of Nd$_2$O$_3$ (Alfa Aesar 99.9%) and ZrO$_2$ (Alfa Aesar 99.7%):

- Added to spherical 3 mm and 10 mm YSZ (yttria stabilized zirconia) milling media in a PTFE (polytetrafluoroethylene) ball mill jar with deionized water and ammonium polyacrylate dispersant (Darvan 821A).
- Milled for 24 hours on the ball mill at 85 rpm.
- Dried in an oven at 120°C.
- Ground with a porcelain mortar and pestle and sieved through a 212 µm stainless steel mesh.
- Calcined at 1350°C for 12 hours.
- Ball milled and dried under the same conditions.

MgO and Nd$_2$Zr$_2$O$_7$ :

- Added to a PTFE ball milling jar containing YSZ milling media with deionized water and ammonium polyacrylate dispersant.
- Milled for 24 hours and dried at 120°C.
- Ground with a porcelain mortar and pestle.

- Sieved through a 212 µm stainless steel mesh.
- Calcined at 1000°C in air for 2 hours.

MgO-$Nd_2Zr_2O_7$ Powder:

- Combined with 2 wt% of binder (20 vol% Celvol 103 Polyvinyl Alcohol in deionized water).
- Ground with an alumina mortar and pestle until the powder sieved through a 300 µm brass mesh.
- Dried in a 120°C oven for 5 minutes.
- Pressed with 68 MPa on a Carver press to form a green body sample.
- Sintered in air at 1550°C for 4 hours.

Fabricated MgO-$Nd_2Zr_2O_7$ pellets:

- Sectioned using a diamond coated blade.
- Ground from 320 grit to 1200 grit diamond abrasive pads.
- Polished with a 1 µm diamond suspension, followed by 0.5 µm colloidal silica.
- Cleaned in an ultrasonic bath.


**Microstructural Characterization**

The microstructure of each phase composition will be analyzed using SEM imaging and ImageJ software. Each sample will be ground from 320 grit paper to 1200 grit paper, then polished to 0.05 µm using a colloidal silica abrasive. After being cleaned in an ultrasonic bath and coated with carbon, three random images will be taken of each sample to be analyzed. The homogeneity of the interpenetrating matrix (the area between heterogeneities in which the two phases are well mixed) will be assigned a dimensionless number $HP_q$ derived using a Voronoi polygon method. The average grain size of each phase in each sample will be determined using lineal analysis. Finally, the contiguity of each phase, meaning the average fraction of grain boundaries at which a grain of a particular phase is self-connected, will be analyzed using lineal analysis.
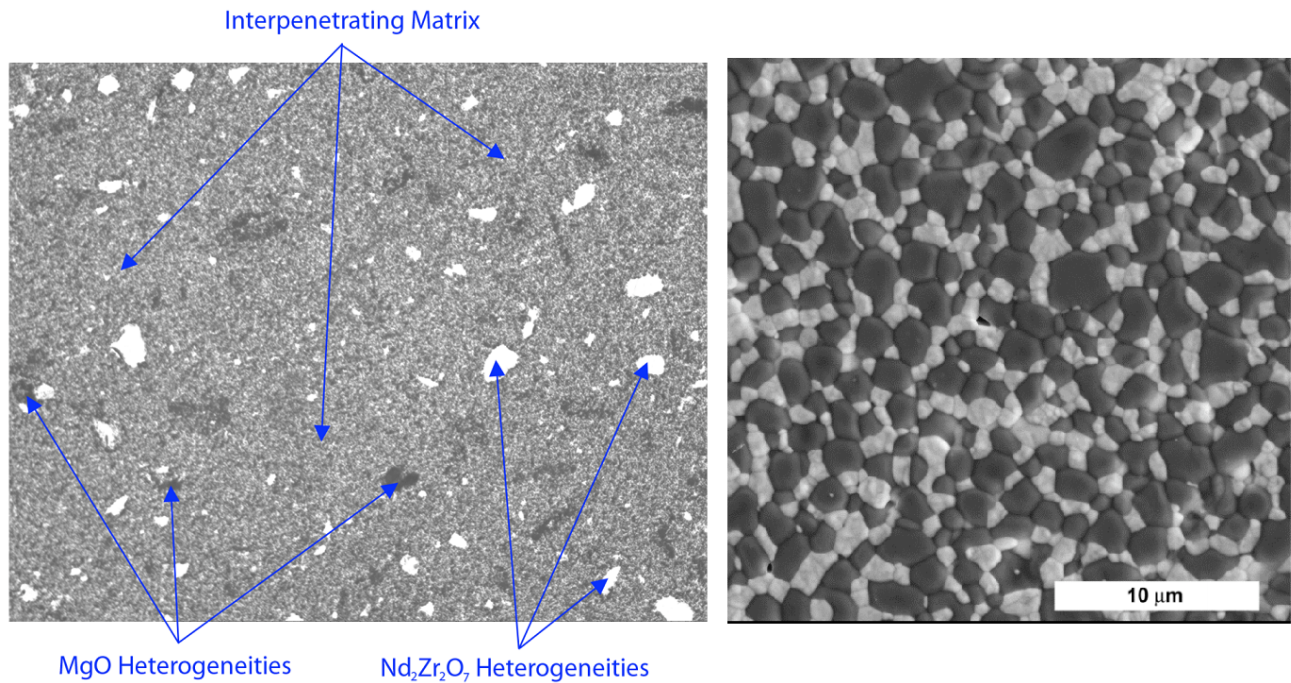
Interpenetrating Matrix



MgO Heterogeneities          $Nd_2Zr_2O_7$ Heterogeneities

**Fig. 5**: Left: the macrostructure of an MgO-$Nd_2Zr_2O_7$ sample. The interpenetrating matrix is analyzed using SEM. Right: the microstructure of an MgO-$Nd_2Zr_2O_7$ composite.

The data gathered from SEM will be used to comment on the relationship between connectivity (the number of dimensions in which a phase is self connected) and thermal conductivity. It is hypothesized that the ideal connectivity for maximum thermal conductivity in a two-phase composite is 3-0, where the MgO phase has a connectivity of 3. This allows heat to flow through the thermally conductive MgO phase while minimizing heat flow impedance by the $Nd_2Zr_2O_7$ phase.

**Thermal Characterization**

The thermal conductivity of each sample from 100°C to 1000°C will be determined using data gathered by a Netzsch laser flash analyzer (LFA). In this process, a laser of known energy is fired at one side of the sample. A thermocouple on the opposite side simultaneously records the objects temperature as a function of time. Once corrected for surface heat loss, sample geometry, and thermal expansion, the thermal diffusivity of the sample can be determined. By multiplying the thermal diffusivity by the material's specific heat capacity and its density,
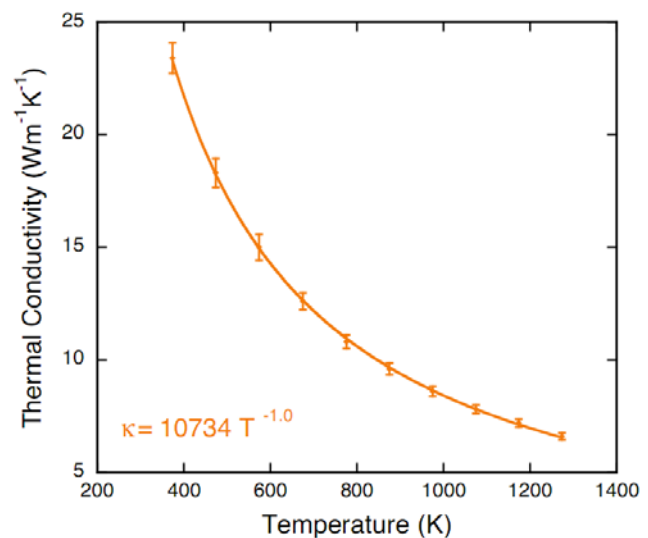


$\kappa = 10734\ T^{-1.0}$

**Fig. 6**: The calculated thermal conductivity of an MgO-$Nd_2Zr_2O_7$composite as a function of temperature.

thermal conductivity is obtained.

The specific heat capacity of each sample will be determined using differential scanning calorimetry (DSC). Measurements are teken in a vacuum furnace at a ramp rate of 20°C/min. Thermal expansion will be quantified using a Netzsch dilatometer. In this process, the sample is heated in a vacuum furnace while changes in its geometry are measured as a function of temperature.

**Progress**

This work is currently in the materials processing stage. Samples have been synthesized, yet due to in error in the milling media used for ball milling, they are well below the target density and are too provide reliable characterization data. New ball mill equipment has been obtained and more samples are currently being fabricated. Excel spreadsheets and ImageJ macros have been developed and will be used to speed the image analysis process once images are obtained.

**Expected Results**

Data gathered in this research will, along with that from previous research on MgO-$Nd_2Zr_2O_7$ composite, result in the determination of the correlation between the phase composition, microstructure, and thermal conductivity of the MgO-$Nd_2Zr_2O_7$ composite. Previous research has shown a correlation between phase composition and connectivity in the MgO-$ZrO_2$ composite, in which the 60 wt% MgO / 40 wt% $ZrO_2$ composition appeared as a dispersion of zirconia in the magnesia phase, while the 40/60 composition was clearly a dispersion of magnesia in the zirconia phase. The 50/50 composition manifested itself as a combination of two interpenetrating phases. Due to the relationship between connectivity and contiguity, it is expected that a proportionality between the vol% of the MgO phase and its contiguity will be observed.
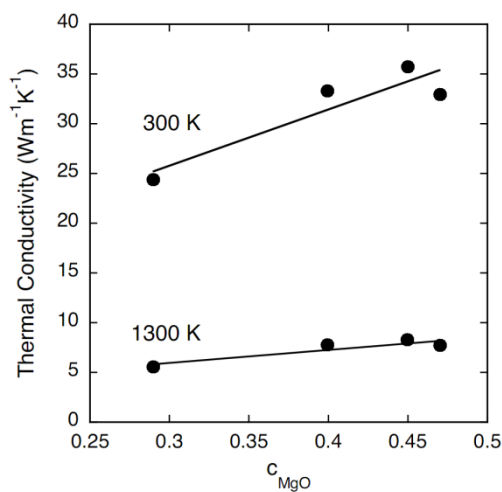


**Fig 7**: The correlation between the contiguity of the MgO phase and the thermal conductivity of the IM material.

Research on the processing of this composite has shown no relationship between grain size or homogeneity and thermal conductivity. This is expected, since neither microstructural property effects connectivity. A clear correlation was observed between the contiguity of the MgO phase and thermal conductivity. If an increase in the vol% of the $Nd_2Zr_2O_7$ phase in the IM material does not lower the contiguity of the MgO phase, such a change in the phase composition will be beneficial, since the hot water corrosion resistance of the material is directly proportional to the vol% of this phase.

Ultimately, this research will allow us to determine the phase composition of the MgO-$Nd_2Zr_2O_7$ composite which yields

the highest thermal conductivity. Furthermore, the data collected will allow others to balance the material's performance in the five criteria it must meet and determine an ideal composition which will be suitable for use in an LWR.